BIOCHEMISTRY
including biophysical chemistry & molecular biology

Article

pubs.acs.org/biochemistry

Insights into the Intramolecular Coupling between the N- and C-Domains of Troponin C Derived from High-Pressure, Fluorescence, Nuclear Magnetic Resonance, and Small-Angle X-ray Scattering Studies

Guilherme A. P. de Oliveira,[†] Cristiane B. Rocha,[‡] Mayra de A. Marques,[†] Yraima Cordeiro,[§] Martha M. Sorenson,[†] Débora Foguel,[†] Jerson L. Silva,*[,†] and Marisa C. Suarez*[,†,∥]

[†]Programa de Biologia Estrutural, Instituto de Bioquímica Médica, Instituto Nacional de Biologia Estrutural e Bioimagem, Centro Nacional de Ressonância Magnética Nuclear Jiri Jonas, Universidade Federal do Rio de Janeiro, 21941-902 Rio de Janeiro, Brazil

[‡]UNIRIO-Universidade Federal do Estado do Rio de Janeiro, CCBS-Centro de Ciências Biológicas e da Saúde, Instituto Biomédico-IB, Departamento de Bioquímica, Rua Frei Caneca 94-Centro, Rio de Janeiro, Brazil

[§]Faculdade de Farmácia, Universidade Federal do Rio de Janeiro, Rio de Janeiro, Brazil

[∥]Programa de Biologia Estrutural, Instituto de Bioquímica Médica-Polo Xerém, Universidade Federal do Rio de Janeiro, Xerém, Brazil

Supporting Information

ABSTRACT: Troponin C (TnC), the Ca^{2+}-binding component of the troponin complex of vertebrate skeletal muscle, consists of two structurally homologous domains, the N- and C-domains; these domains are connected by an exposed α-helix. Mutants of full-length TnC and of its isolated domains have been constructed using site-directed mutagenesis to replace different Phe residues with Trp. Previous studies utilizing these mutants and high hydrostatic pressure have shown that the apo form of the C-domain is less stable than the N-domain and that the N-domain has no effect on the stability of the C-domain [Rocha, C. B., Suarez, M. C., Yu, A., Ballard, L., Sorenson, M. M., Foguel, D., and Silva, J. L. (2008) *Biochemistry* 47, 5047−5058]. Here, we analyzed the stability of full-length F29W TnC using structural approaches under conditions of added urea and hydrostatic pressure denaturation; F29W TnC is a fluorescent mutant, in which Phe 29, located in the N-domain, was replaced with Trp. From these experiments, we calculated the thermodynamic parameters (ΔV and ΔG°_{atm}) that govern the folding of the intact F29W TnC in the absence or presence of Ca^{2+}. We found that the C-domain has only a small effect on the structure of the N-domain in the absence of Ca^{2+}. However, using fluorescence spectroscopy, we demonstrated a significant decrease in the stability of the N-domain in the Ca^{2+}-bound state (i.e., when Ca^{2+} was also bound to sites III and IV of the C-domain). An accompanying decrease in the thermodynamic stability of the N-domain generated a reduction in $\Delta\Delta G^{\circ}_{atm}$ in absolute terms, and Ca^{2+} binding affects the Ca^{2+} affinity of the N-domain in full-length TnC. Cross-talk between the C- and N-domains may be mediated by the central helix, which has a smaller volume and likely greater rigidity and stability following binding of Ca^{2+} to the EF-hand sites, as determined by our construction of low-resolution three-dimensional models from the small-angle X-ray scattering data.

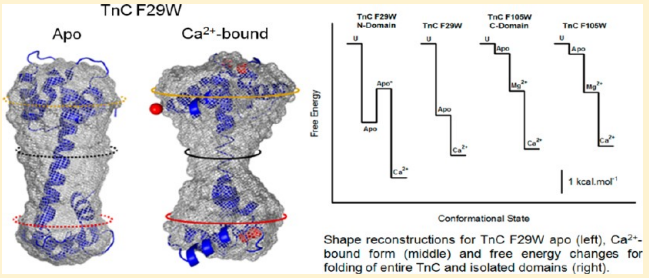

Shape reconstructions for TnC F29W apo (left), Ca^{2+}-bound form (middle) and free energy changes for folding of entire TnC and isolated domains (right).

Troponin C (TnC) is a Ca^{2+}-binding protein in skeletal and cardiac muscles. Like troponins I and T and tropomyosin, TnC is involved in thin-filament regulation of muscle contraction and relaxation. The X-ray diffraction of skeletal muscle TnC crystals reveals an elongated dumbbell-shaped structure with two globular domains that are at the N- and C-termini. These domains are connected by an exposed α-helix that is flexible in solution.[1−6] The N-terminal domain of TnC has two sites (I and II) with a low affinity for Ca^{2+} ($K_{a[Ca]} = 3.2 \times 10^5\ M^{-1}$), whereas sites III and IV in the C-domain have a high affinity for Ca^{2+} ($K_{a[Ca]} = 2 \times 10^7\ M^{-1}$). Sites III and IV also bind Mg^{2+} ($K_{a[Mg]} = 5 \times 10^3\ M^{-1}$). In addition to sites III and IV, the C-terminal domain also harbors weak sites that bind Mg^{2+} as well as Ca^{2+} with very low affinity ($K_{a[Ca,Mg]} \sim 10^2-10^3\ M^{-1}$).[7−11] In vivo, the initiation of contraction occurs when Ca^{2+} ions bind to sites I and II, whereas sites III and IV within the C-domain are likely constantly occupied by Ca^{2+} or Mg^{2+}, allowing these sites to play a structural role. Binding of Ca^{2+} or Mg^{2+} to the weak sites of the C-domain of TnC induces exposure of a large hydrophobic surface that leads to the release of TnC from the thin filament.[11]

Received: August 22, 2012
Revised: December 5, 2012
Published: December 7, 2012

ACS Publications © 2012 American Chemical Society

Several studies have been performed to explain the differences in the affinity of Ca^{2+} for the N- and C-domains. As expected, the affinity of these domains for Ca^{2+} depends on the amino acid sequence of the Ca^{2+}-binding loop.[12−14] Long-range interactions can also affect the affinity of these domains for Ca^{2+}. In the C-domain of chicken TnC, replacing Thr with Ile at position 130 decreases Ca^{2+} affinity by a factor of 2.5; the mutation site is more than 20 Å from divalent cation-binding sites III and IV.[15] Removal of the N-helix (11 amino acids that precede helix A at the N-terminus) significantly reduces the Ca^{2+} affinity of the N-domain.[16] Introduction of covalent or ionic links between adjacent helices at positions distant from the Ca^{2+}-coordinating residues renders the N-domain less able to open upon Ca^{2+} binding, and it decreases the affinity for Ca^{2+}.[17,18] Gagné and colleagues[14] demonstrated that an N-domain that remains closed after binding Ca^{2+} has an affinity reduced by a factor of 100-fold. Conversely, TnC mutants that favor the opening of a hydrophobic cleft in the N-domain have an increased affinity for Ca^{2+}.[19,20]

In 1996, Fredricksen and Swenson[21] proposed that the affinity for Ca^{2+} is determined by the thermodynamic stability of the protein when the protein stability is measured in the absence of divalent cations. In fact, the C-domain has a lower stability than the N-domain in the absence of added cations. Glycerol, an osmolyte that induces stabilization and a "locked" conformation of the N-domain, decreases its affinity for Ca^{2+}.[22]

Fluorescence spectroscopy has been used extensively in studies of protein folding to determine changes in the tertiary and quaternary structures of proteins.[23] Chicken skeletal muscle TnC is devoid of Trp or Tyr in its primary sequence. However, using a Trp mutant of the isolated C-domain (F105W/C-domain, residues 88−162) as well as the intact TnC with the same mutation (F105W), we were able to evaluate the stability of the isolated C-domain and compare it to the intact protein.[24] Position 105 faces site III in the C-domain,[25,26] and W105 serves as a probe for conformational changes in this region of the protein. Combining hydrostatic pressure (in the range of 1−3100 bar) with subdenaturing concentrations of urea,[24] we confirmed the low stability of the apo form of the C-domain; we also found that binding of Ca^{2+} markedly stabilizes the structure of this domain. Interestingly, we also observed that the N-domain of TnC has practically no effect on the structure of the C-domain, even in the presence of Ca^{2+}.

In addition to the F105W mutants, other replacements of Phe residues with Trp have been exploited.[19,27−29] The F29W TnC mutant was first constructed as a spectral probe in 1992.[19] This mutant has been extensively characterized in solution and in skinned fibers. Like other Trp and Tyr constructs, F29W TnC is not a perfect surrogate for the wild-type protein. Among these mutants (at positions 22, 29, 48, 52, 78, and 90),[19,28,29] F29W provides the strongest fluorescence signal. The regulatory sites of the wild-type recombinant protein have the same affinity and apparent cooperativity for Ca^{2+} as the native chicken protein (for the recombinant protein, pCa_{50} = 5.6 and n_H = 1.8, and for the native chicken protein, pCa_{50} = 5.6 and n_H = 1.7), as well as the same secondary structure content with and without Ca^{2+}.[15] The F29W TnC mutant differs slightly from the wild-type recombinant protein at submaximal Ca^{2+} levels (pCa_{50} = 5.7, and n_H = 2.0), but the changes in ellipticity with or without Ca^{2+} were initially considered to be identical.[19] It is noteworthy that in all of these assays, the isolated F29W/N-domain (residues 1−90) behaved exactly like the full-length mutant protein,[26] and this is important for the experimental approach that we utilize. In addition, of course, it provides an excellent fluorescent signal for the N-domain, a 3-fold increase in the presence of Ca^{2+} with a <10% contribution[30] from C-domain sites.

Functionally, the F29W mutant and wild-type recombinant chicken proteins behave identically in skinned fibers, where they restore the same maximal isometric force, Ca^{2+} sensitivity, apparent cooperativity, and affinity for the thin filament.[16] In ATPase assays with reconstituted thin filaments, both proteins restore Ca^{2+} affinity, although the F29W TnC mutant is deficient in maximal activation (43% of the value obtained using the wild-type recombinant protein). This observation suggests interference in the interaction of TnC with TnI or TnT.[16] Neither the F22W mutant nor the F52W mutant exhibits this problem, although they exhibit weaker Ca^{2+} binding signaling.[28]

Possible structural correlates that could account for differences between the mutant and wild-type recombinant N-domains were examined in the apo forms using ^1H NMR and molecular modeling.[31] There was evidence of adjustments in Ca^{2+}-binding loop I (residues 30−38) to accommodate the bulkier Trp residue. The mutant seemed to have more internal cavity space, making it more compressible at very high pressures (5 kbar) and less stable (with thermal denaturation beginning at 47 °C rather than 56 °C). These changes would be expected to affect the N-domain and the full-length protein similarly.

Here, we investigate whether the C-domain affects the N-domain structure. Using two mutant proteins (F78W and F154W) to determine the thermal stability of intact TnC, Moncrieffe and colleagues[29] observed that the stability of the apo form of the N-domain increases when Mg^{2+} is bound to sites III and IV of the C-domain and decreases when Ca^{2+} is bound to these sites. Recently, rapid pressure jump and stopped-flow techniques have shown that binding of Mg^{2+} to the C-domain of the F29W TnC mutant inhibits binding of Ca^{2+} to sites I and II.[32]

In our study, we studied the intact F29W TnC mutant using structural approaches, including small-angle X-ray scattering (SAXS), fluorescence spectroscopy, and nuclear magnetic resonance (NMR). With these techniques, we obtained thermodynamic parameters of folding for F29W TnC and compared these values with those previously obtained for the isolated F29W/N-domain.[33] As determined by the Gibbs free energy change of the full-length F29W TnC and F29W/N-domain,[33] we observed that the apo form of the C-domain has no significant effect on the thermodynamic stability of the apo form of the N-domain (from −3.4 to −3.11 kcal/mol). However, we observed that the C-domain significantly decreases the stability of the N-domain (from −5.82 to −4.85 kcal/mol) when all four sites of TnC (I−IV) are occupied by Ca^{2+}. The intramolecular coupling between the C- and N-domains following Ca^{2+} binding may be mediated by the central helix, which has a smaller volume and likely becomes more rigid and stable as determined by SAXS experiments. Cumulatively, these findings reveal new information about the complex interaction between the N- and C-domains of TnC, and they raise the possibility that Ca^{2+}−Mg^{2+} equilibria at sites III and IV may alter the response to Ca^{2+} binding in the N-domain.

dx.doi.org/10.1021/bi301139d | Biochemistry 2013, 52, 28−40

EXPERIMENTAL PROCEDURES

Sample Preparation. Trp was introduced into the cDNA of recombinant chicken skeletal muscle TnC by site-directed mutagenesis, replacing Phe at position 29. The C-domain in both recombinant proteins (wild-type and F29W) carries a spontaneous mutation from Thr to Ile at position 130, which reduces the Ca^{2+} affinity (pCa_{50}) of sites III and IV from 7.1 to 6.7; no change in n_H was observed (1.8 and 1.9). These proteins begin with Met and are not acetylated at the N-terminus.[15] The F29W TnC protein was expressed in *Escherichia coli* BL21 cells and extracted and purified as previously described.[26]

Small-Angle X-ray Scattering (SAXS). SAXS data were collected with the SAXS2 small-angle scattering beamline of the National Synchrotron Light Laboratory (Campinas, Brazil) using a two-dimensional MARCCD detector with a mica sample holder, a wavelength (λ) of 0.155 nm, and a temperature of 25 °C. Experiments were performed in standard buffer [20 mM Tris-HCl (pH 7.0) and 0.1 mM DTT and the corresponding conditions to be tested: 1.5 mM EGTA, 1.5 mM EGTA with 4 M urea, 2.1 mM $CaCl_2$, or 2.1 mM $CaCl_2$ with 7 M urea]. The protein concentration ranged from 477 μM (8.62 mg/mL) to 494 μM (8.95 mg/mL). Data were acquired by taking two frames of 300 s for each sample. The modulus of scattering vector q was calculated according to the equation $q = (4\pi/\lambda) \sin \theta$, where λ is the wavelength used and 2θ is the scattering angle. The sample−detector distance was set at 973.77 mm, allowing detection of q in a range from 0.14 to 3.5 nm^{-1}. The monodispersity of the samples was confirmed by Guinier plots of the data. Data were corrected properly and fit using GNOM,[34] and the low-resolution ab initio particle shape was restored using GASBOR.[35] The final model was the result of an average of 10 independent calculations, performed using DAMAVER.[36] Superposition of the high-resolution crystal structures of TnC [Protein Data Bank (PDB) entries 1TCF and 1NCZ] and the molecular envelopes of the apo and Ca^{2+}-bound forms and Ca^{2+}-bound form treated with 7 M urea were obtained by the best fit using SUPCOMB.[37] Because we were not able to obtain the best fit using the SUPCOMB minimization software for the apo form treated with 4 M urea, we employed a manual adjustment using the PyMOL Executable Build software (PyMOL Molecular Graphics System, version 0.99, Schrödinger, LLC).

Dynamic Light Scattering (DLS). DLS measurements were performed on a Brookhaven (Holtsville, NY) 90Plus/Bi-Mas multiple-angle particle sizing instrument. Data were analyzed using multimodal size distribution (MSD) software. The MSD feature takes the autocorrelation function and uses a non-negatively constrained least-squares (NNLS) algorithm to produce an intensity-weighted differential size distribution. Results are shown by number-weighted distribution. Each measurement consisted of three independent readings, and each was 30 s in duration. The protein concentration was 424.5 μM, and buffer conditions were the same as those used for SAXS. Samples were incubated at room temperature for 1 h, centrifuged at 10000g for 10 min at 4 °C, and filtered (0.22 μm) prior to the measurement at 25 °C.

High-Pressure Nuclear Magnetic Resonance (HP NMR). HP HSQC spectra were acquired using a zirconium high-pressure cell system (Daedalus Innovations) at 25 °C with a Bruker Avance III 800 MHz spectrometer. HSQC spectra were recorded at 1, 1000, and 2500 bar and after decompression, with 10 min intervals following each increase in pressure. The protein concentration was 150 μM, and the buffer conditions were as follows: 20 mM Tris-HCl containing 0.1 mM DTT and 2.1 mM $CaCl_2$ in the presence or absence of 5 or 7 M urea. All samples were analyzed at 1 bar or at HP, and they were incubated at room temperature for 16 h prior to measurements.

Fluorescence Studies under Pressure. The high-pressure cell has been described by Paladini and Weber.[38] The experiments were performed under pressure in standard buffer [100 mM Tris-HCl, 100 mM KCl, 1.0 mM DTT, and 1.5 mM EGTA (pH 7.0)] at 20 °C. The Trp fluorescence spectra were recorded on an ISSK2 spectrofluorometer (ISS Inc., Champaign, IL). The sample was excited at 280 nm, and emission was collected between 300 and 400 nm in a 1 cm square cuvette without stirring. Fluorescence spectra were quantified as the center of spectral mass (υ_p)

$$\upsilon_p = \sum \upsilon_i F_i / \sum F_i \quad (1)$$

where F_i stands for the fluorescence emitted at wavenumber υ_i and the summation is conducted over the range of appreciable values of F.

The degree of denaturation under a given condition (α) was calculated from the center of spectral mass under that condition (υ) by

$$\alpha = (\upsilon_i - \upsilon)/(\upsilon_i - \upsilon_f) \quad (2)$$

where υ_i and υ_f represent the initial and the final values for the center of spectral mass (native and unfolded protein), respectively.

After each increase in pressure in a given sequence, the spectrum was recorded after 5 min to allow for equilibration. The protein concentration was 5 μM for all measurements. All spectroscopic changes reported were completely reversible.

Thermodynamic Parameters. The degree of denaturation (α) at pressure p is related to the volume change for this process by the thermodynamic relationship given below:[39]

$$\ln(\alpha/1 - \alpha) = (\Delta V/RT)p + \ln K_{atm} \quad (3)$$

The volume change (ΔV) can be calculated from the slope of this plot. The Gibbs free energy change at atmospheric pressure in the absence of urea (ΔG°_{atm}) is calculated from the following equation:

$$\Delta G^{\circ(U)}{}_{1241} = m(U) + \Delta G^{\circ 0M}{}_{1241} \quad (4)$$

where m is the difference in solvent-accessible surface area as the protein unfolds in the presence of different concentrations of urea (U) and $\Delta G^{\circ 0M}{}_{1241}$ is the free energy change at 1241 bar in the absence of urea. Values of $\Delta G^{\circ 0M}{}_{1241}$ obtained in the presence or absence of Ca^{2+} were introduced into eq 5 to determine the free energy change at atmospheric pressure (ΔG°_{atm}).

$$\Delta G^{\circ 0M}{}_{1241} = \Delta G^\circ{}_{atm} + p\Delta V \quad (5)$$

RESULTS

SAXS and HSQC Experiments: Conformational Changes of F29W TnC Induced by Ca^{2+} and Urea. Previous experiments comparing the isolated N- and C-domain mutants of TnC with the full-length protein show that the fluorescence signals from Trp 29 and Trp 105 faithfully report events in the N- and C-domains, respectively. These events are

dx.doi.org/10.1021/bi301139d | *Biochemistry* 2013, 52, 28−40

not contaminated by cross-talk from the other end of the molecule.[26] In our previous work, we evaluated the stability of the F105W/C-domain and compared it to the intact protein (F105W TnC). We observed that in the presence of urea alone or upon combination of hydrostatic pressure (range of 1−3100 bar) with subdenaturing concentrations of urea, the N-domain of TnC has practically no effect on the structure of the C-domain, even in the presence of Ca^{2+}.[24]

To obtain more information about the concomitant conformational changes induced in the N- and C-domains of F29W TnC by Ca^{2+} and urea, we designed a set of experiments using SAXS. After obtaining the scattering curves $I(q)$ (Figure S1 of the Supporting Information), we were able to calculate the radii of gyration (R_g) from the linear regression along the low-q region of the Guinier plots (Figure S2 of the Supporting Information). Guinier plot linearity and size distribution by DLS measurements (Figure S3 of the Supporting Information) were assessed to guarantee the monodispersity of samples. A nonlinear Guinier plot is a strong indicator of polydisperse samples. Samples containing significant nonspecific aggregates yield Guinier plots with a sharp increase in intensity at very small values of q. None of the calculated Guinier plots obtained by SAXS showed increased intensity at small values of q (see Figure S2 of the Supporting Information). The same conditions used for the SAXS experiments were also used in DLS experiments, confirming a narrow size distribution (see Figure S3 of the Supporting Information). The pair-distance distribution function $P(r)$ of interatomic vectors, calculated with GNOM,[34] also provided R_g values (Table 1). The $P(r)$ function allows for the graphic display of the peculiarities of the particle shape.[40] For instance, globular particles yield bell-shaped profiles, and multidomain particles often yield profiles with multiple shoulders and oscillations corresponding to intra- and interdomain distances. Our SAXS data clearly revealed a prominent shoulder in the $P(r)$ function of the Ca^{2+}-bound state of F29W TnC that was not present in the apo form (Figure 1A). Moreover, the addition of 4 M urea to the apo form shifted the $P(r)$ function to a broader, bell-shaped profile, which is evidence of the partial denaturation of the structure. We also observed that in the presence of 4 M urea, the apo form expanded to a greater maximal diameter [D_{max} (Table 1)], indicating an extended, unfolded conformation. However, the dimensions of the F29W TnC Ca^{2+}-bound form changed only slightly upon addition of 7 M urea (Table 1). To evaluate protein folding, the Kratky plot is useful.[41] Typically, folded globular proteins yield a single prominent peak in the Kratky plot, whereas unfolded proteins exhibit a continuous increase in the product of scattering intensity times q^2 versus q. Our Kratky results for F29W TnC revealed a more prominent peak for the Ca^{2+}-bound form than for the apo form (Figure 1B), an indication that Ca^{2+} binding leads to a populated folded state. Treatment of the apo form with 4 M urea led to a monotonic Kratky plot, typical of an unfolded protein; this plot contrasted the biphasic profile of the plot for the Ca^{2+}-bound state treated with 7 M urea (Figure 1B).

Table 1. Molecular Parameters Obtained by SAXS and DLS

sample	Guinier R_g (Å)[a]	GNOM R_g (Å)	D_{max} (Å)	D_h (Å)
apo	25.1	18.3	60	33 ± 2
apo with 4 M urea	39	31.3	90	67 ± 5
Ca^{2+}	19.2	22	61	45 ± 1
Ca^{2+} with 7 M urea	24	24.3	70	72 ± 6

[a] R_g was obtained from the angular coefficient (α) of the linear regression of the Guinier domain (Figure S2 of the Supporting Information) via $\alpha = R_g^2/3$.

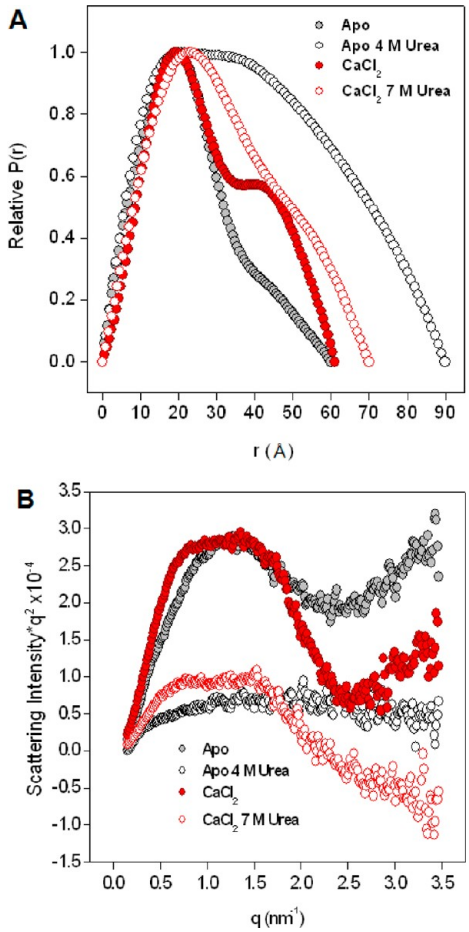

Figure 1. (A) Pair-distance distribution functions of interatomic vectors [$P(r)$] obtained from the scattering intensities (Figure S1 of the Supporting Information) and (B) Kratky plots.

The reconstruction of low-resolution three-dimensional (3D) models from SAXS data is a rapid and powerful tool for inferring structural changes in proteins. We analyzed our scattering data with GASBOR, which generates ab initio models using simulated annealing strategies.[42] The final models for each condition are shown in Figure 2. The consensus shape reconstruction for the F29W TnC apo form (Figure 2A) and the Ca^{2+}-bound form (Figure 2B) matched the crystal structures of TnC PDB entries 1NCZ and 1TCF, respectively. Although comparison of the apo and Ca^{2+}-bound states did not reveal significant changes in R_g and D_{max} [18.3 and 22 Å for R_g and 60 and 61 Å for D_{max}, respectively (Table 1)], model reconstructions using GASBOR clearly reveal a difference in the envelope density for each condition (Figure 2A,B). These differences are confirmed by hypothetical circumferences; Ca^{2+} led to a broader volume for the N- and C-domains compared to that of the apo form. The envelope density of F29W TnC in the absence of cations also revealed a prolate shape with additional density in the central helix (Figure 2A) compared to the Ca^{2+}-bound form, which has the shape of an hourglass (Figure 2B). The extra volume surrounding the central helix in the apo form presumably is due to the apo form of TnC

dx.doi.org/10.1021/bi301139d | Biochemistry 2013, 52, 28−40

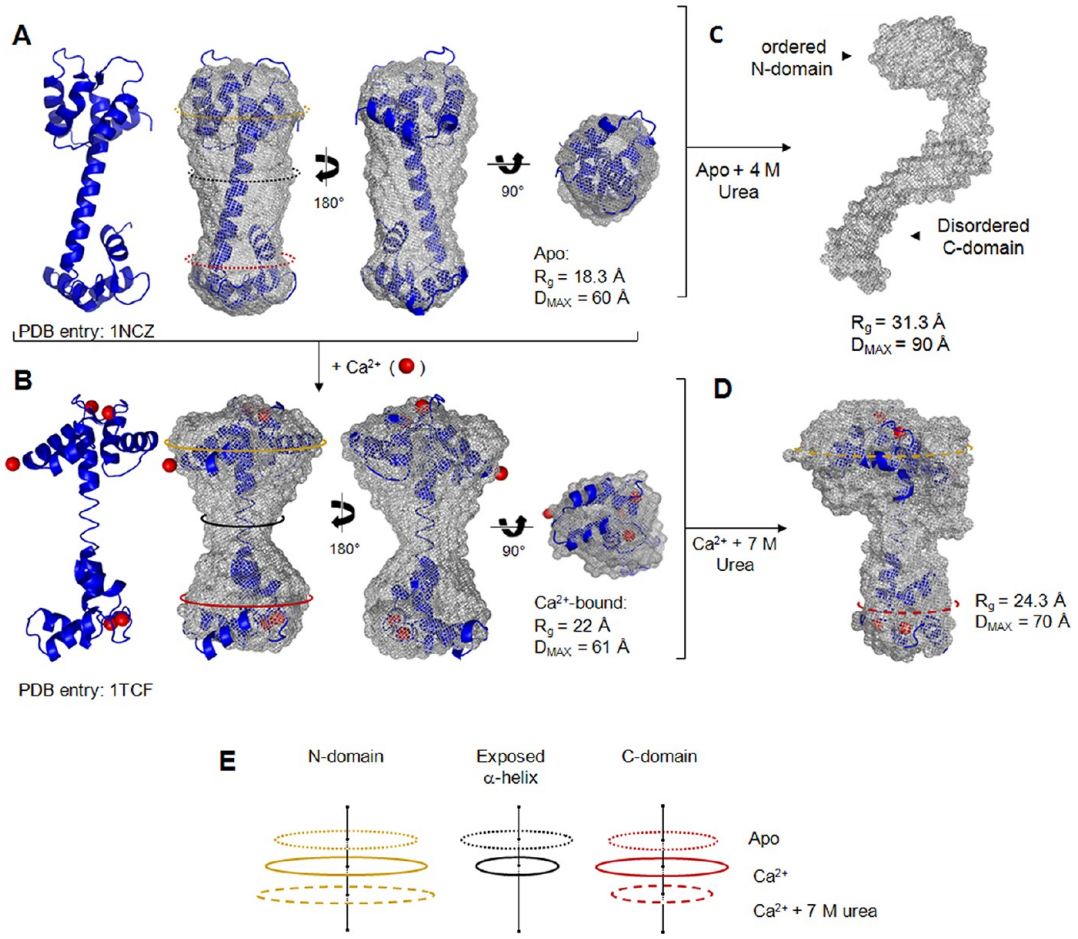

Figure 2. SAXS reconstruction models for the apo and Ca^{2+}-bound forms of F29W TnC in the presence or absence of urea. (A) Ribbon representation of the high-resolution TnC crystal structure (PDB entry 1NCZ) colored blue (left). Molecular envelope reconstructions of the apo form (gray mesh) superimposed with the crystal structure of TnC (blue), differing by a 180° vertical rotation (middle) and a 90° horizontal rotation (right). (B) Ribbon representation of the high-resolution crystal structure of the TnC Ca^{2+}-bound form (PDB entry 1TCF) colored blue (left). Molecular envelope reconstructions (gray mesh) for the Ca^{2+}-bound state of F29W TnC as shown in panel A. (C) Molecular envelope reconstruction of the apo form treated with 4 M urea, showing the unfolding of the C-domain and the retained globular structure of the N-domain (arrowheads). (D) Molecular envelope reconstruction of the Ca^{2+}-bound state treated with 7 M urea superimposed on the crystal structure of the Ca^{2+}-bound state. (E) Changes in the molecular envelope diameter in three different regions of the protein depicted as hypothetical circumferences obtained from the reconstructed models derived from the GNOM and GASBOR analyses of the $I(q)$ plots. Dotted lines are shown for the apo form, solid lines for the Ca^{2+}-bound state, and dashed lines for the Ca^{2+}-bound state treated with 7 M urea. The N-domain, central helix, and C-domain are colored gold, black, and red, respectively.

populating a wide range of heterogeneous conformations. When Ca^{2+} binds, the central helix apparently loses its flexibility and becomes more rigid (as observed by the constricted waist in the Ca^{2+}-bound form).

The addition of 4 M urea to the apo form led to a significant change in R_g and D_{max} values compared to those of the nontreated apo form. When 4 M urea is present, the R_g and D_{max} values for the F29W TnC apo form increase ~71 and 50%, respectively [from 18.3 to 31.3 Å and from 60 to 90 Å, respectively (Table 1)]. These changes were confirmed in the molecular reconstruction by denaturation of part of the structure (Figure 2C). In this case, we were not able to determine the best superposition fit using SUPCOMB (see Experimental Procedures); thus, we performed a manual adjustment of the TnC crystal structure to allow the structure to fit into the shape reconstruction of the apo form treated with 4 M urea. This procedure led to a reasonable fit between the ordered density and the N-domain of the TnC crystal structure (Figure S4 of the Supporting Information). Thus, we believe that this ordered region corresponds to the N-domain, while the disordered region corresponds to the disassembled C-domain. We infer that the C-domain of the apo form is very unstable and is not involved in providing stability to the N-domain structure. Several other orientation trials using the crystal structure and the SAXS reconstruction were performed in this way, and none of the trials led to a coherent superposition.

With respect to the F29W TnC Ca^{2+}-bound form, the R_g and D_{max} values increased slightly after the addition of 7 M urea (~10 and 15%, respectively), suggesting a large stabilizing effect of Ca^{2+} (Table 1). However, as shown in Figure 2E, the hypothetical circumference of the N-domain increases while that of the C-domain decreases (Figure 2E). These results suggest that the difference in R_g values between the F29W TnC Ca^{2+}-bound form and this form in the presence of 7 M urea arises because of structural changes in the N-domain. Hydrodynamic diameters (D_h) obtained by DLS (Table 1) were consistent with the SAXS data, i.e., twice as large as the

dx.doi.org/10.1021/bi301139d | *Biochemistry* 2013, 52, 28−40

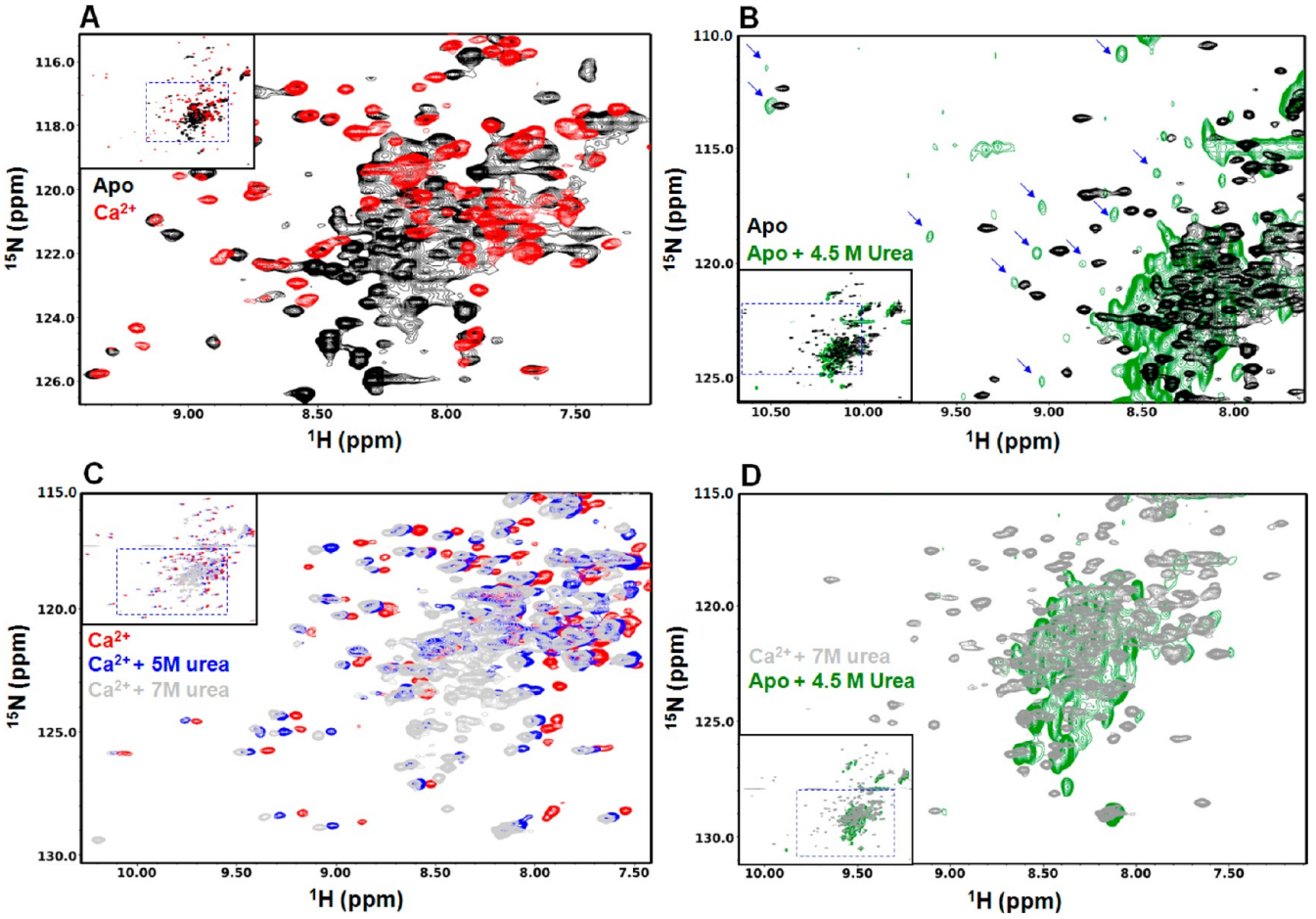

Figure 3. (A–D) HSQC spectra under various conditions for the apo and Ca^{2+}-bound states of F29W TnC. Insets show the full spectra for all conditions. Blue dashed squares show the highlighted region. Blue arrows in panel B show where the well-dispersed peaks are maintained following treatment of the apo form with 4.5 M urea. In panel C, regardless of the systematic shift to the left caused by the presence of urea, note that the peak dispersions of the Ca^{2+}-bound form are very similar in the absence and presence of urea.

values of R_g obtained by SAXS in the apo form (R_g = 18.3 Å, and D_h = 33 Å), the Ca^{2+}-bound form (R_g = 22 Å, and D_h = 45 Å), and the apo form treated with 4 M urea (R_g = 31.3 Å, and D_h = 67 Å). For the Ca^{2+}-bound form treated with 7 M urea, the R_g and D_h values were quite different (24.3 and 72 Å, respectively) possibly because of hydration effects in the N-domain.

Additionally, we performed HSQC NMR experiments to provide more accurate information about the stability of the F29W TnC Ca^{2+}-bound form. Comparison of HSQC spectra for the apo and Ca^{2+}-bound proteins revealed a large cluster of severely overlapped cross-peaks around the middle of the spectrum of the apo form in contrast to the well-dispersed profile of the Ca^{2+}-bound form (Figure 3A). The treatment of the apo form with 4.5 M urea led to the disappearance and intensity reduction of previously well-dispersed cross-peaks of the untreated apo form, but some of the cross-peaks were still well-dispersed (Figure 3B, blue arrows). Additionally, the overlapped region in the middle of the spectrum was increased following addition of urea (Figure 3B). This result shows that the apo form maintains a residual ordered structure upon addition of 4.5 M urea. Conversely, the HSQC spectrum of the Ca^{2+}-bound state was clearly not affected by the treatment with 5 and 7 M urea: except for a systematic shift in position caused by the presence of urea, the well-dispersed peaks were maintained (Figure 3C). The comparison between the HSQC spectrum of the apo form treated with 4.5 M urea and that of the Ca^{2+}-bound form treated with 7 M urea indicated a more disordered structure in the apo form (Figure 3D). Unfortunately, we were unable to perform 3D NMR experiments to obtain information for mapping cross-peak changes in HSQC spectra of the apo and Ca^{2+}-bound states of F29W TnC.

Fluorescence Measurements. The intrinsic fluorescence of F29W TnC was used to observe the conformational changes induced by Ca^{2+} and urea and to calculate the thermodynamic parameters (ΔV and ΔG°_{atm}) that govern the folding of intact F29W TnC in the presence or absence of Ca^{2+}. As shown in Figure 4A, Ca^{2+} promotes a 3-fold increase in Trp 29 emission at 336 nm, indicating that Trp 29 now samples an environment where some internal quenching is reduced. In addition to fluorescence intensity, the spectral distribution of the Trp emission, expressed by the average wavenumber (center of spectral mass, cm^{-1}), can supply a quantitative index of the Trp environment. In Figure 4B, we show the spectral distribution for F29W and F105W TnC. In the apo form of F29W TnC, the average energy of the emission was 29061 cm^{-1}. However, the center of spectral mass of the F105W apo form is observed at 28548 cm^{-1}, a value close to the maximum observed for free Trp in solution.[23] This lower value suggests that Trp 105 is extremely exposed to the solvent and lies in a region near site III that is almost devoid of tertiary contacts. Interestingly, consistent with the SAXS models (Figure 2C), the values for

dx.doi.org/10.1021/bi301139d | Biochemistry 2013, 52, 28–40

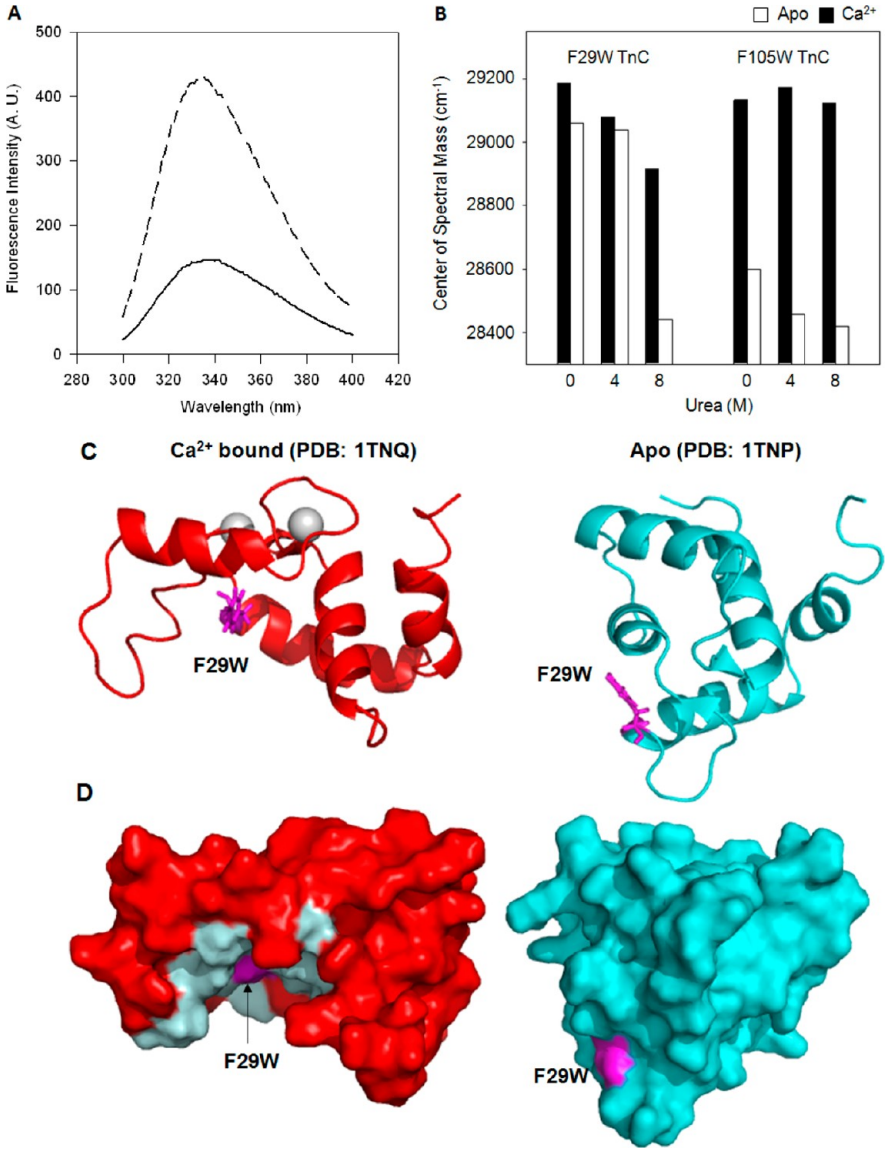

Figure 4. (A) Tryptophan emission spectra of F29W TnC in the presence (– – –) and absence of 2.1 mM $CaCl_2$ (—). (B) Spectral distribution of Trp emission, expressed as the average wavenumber (center of spectral mass, cm^{-1}) of F29W TnC and F105W TnC in the presence (black bars) or absence (white bars) of 2.1 mM $CaCl_2$ following treatment with 0, 4, and 8 M urea. (C) Ribbon representation for the N-domain of TnC in the Ca^{2+}-bound form (red) and apo form (cyan). The F29W mutation is depicted as sticks (magenta). Ca^{2+} ions are highlighted as gray spheres. (D) Surface representation of structures depicted in panel C showing the highly hydrophobic core (light cyan) in which F29W is surrounded following Ca^{2+} binding.

the center of spectral mass with 4 M urea revealed that the structure of the N-domain (reported by Trp 29) was not significantly affected. This result contrasted with the C-domain (reported by Trp 105), which was completely unfolded under identical conditions. These effects were confirmed by adding higher concentrations of urea. The center of spectral mass for the F105W apo form in the presence of 8 M urea was very similar to that obtained in the presence of 4 M urea. Additionally, the complete denaturation of the apo form of the N-domain was attained in the presence of up to 6 M urea[33] (Figure 4B).

The addition of Ca^{2+} induced a blue shift in the fluorescence spectra of F29W TnC and F105W TnC (Figure 4B, black bars at 0 M urea). These shifts indicate that the Trp residues were both less exposed to the solvent and suggested that Ca^{2+} binding promoted larger structural changes in the C-domain of TnC, as reported by Trp 105. The surface representation of the TnC apo form of the N-domain and the Ca^{2+}-bound state confirmed that F29W clustered into a highly hydrophobic core upon Ca^{2+} binding (Figure 4C,D). We also observed that the center of spectral mass of F105W TnC was unaffected in the presence of 8 M urea[24] (Figure 4B), suggesting the absence of conformational changes in the C-domain (see Figure 2D). However, the center of spectral mass of F29W TnC decreased to 270 cm^{-1}. These results suggest that 8 M urea had an effect only on the structure of the N-domain. It is important to note that in the presence of Ca^{2+} at atmospheric pressure, 8 M urea promoted a larger decrease in the center of spectral mass of the intact F29W TnC when compared to the isolated N-domain[33] (Table 2). This variation reveals that the Ca^{2+}-bound state of the C-domain modulated the conformation of the Ca^{2+}-bound N-domain.

dx.doi.org/10.1021/bi301139d | *Biochemistry* 2013, 52, 28–40

Table 2. Centers of Spectral Mass (cm^{-1}) of F29W TnC and F29W/N-Domain in the Ca^{2+}-Bound State (2.1 mM $CaCl_2$) in the Absence or Presence of 8 M Urea

	0 M urea	8 M urea	Δcm^{-1}
F29W TnC	29185	28915	−270
F29W/N-domain	29104	29116	12

Pressure Experiments. Our SAXS and NMR data revealed insights about the overall stability of the TnC F29W mutant and the two lobes separately. To make a complete thermodynamic characterization of the denaturation of F29W TnC, particularly in the presence of Ca^{2+}, we utilized hydrostatic pressure techniques. High-pressure studies have been valuable for studying protein denaturation, protein dissociation, and protein−ligand interactions.[43−47] In panels A and B of Figure 5, we show the effect of pressure on the F29W TnC apo and Ca^{2+}-bound forms, respectively. In the absence of urea [Figure 5A,B (○)], there was only a small red shift in the center of spectral mass at 3.1 kbar. This effect indicates incomplete denaturation of the protein induced by high pressure. To obtain the thermodynamic parameters (ΔV and ΔG°_{atm}) for folding of F29W TnC in the presence or absence of Ca^{2+}, we employed a combination of high hydrostatic pressure and different concentrations of urea to shift the equilibrium toward the unfolded state. Increasing urea concentrations facilitated the unfolding of F29W TnC, as revealed by the decrease in the center of spectral mass. In the absence of Ca^{2+} (Figure 5A), the concentration of urea needed to promote complete unfolding under high-pressure conditions was lower than the concentration needed to denature the Ca^{2+}-bound state (Figure 5B).

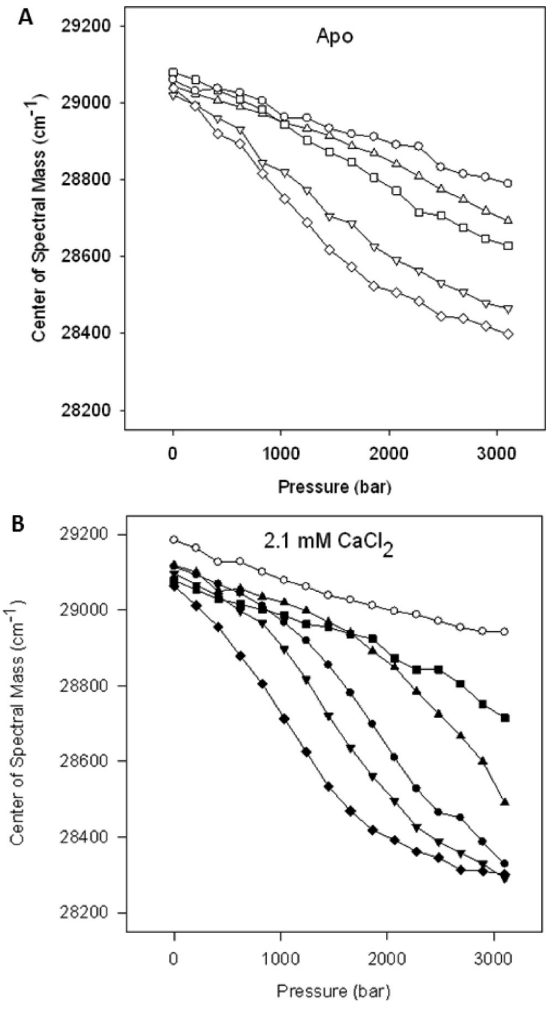

Figure 5. (A) Pressure-induced denaturation of the F29W TnC apo state, in the presence of 2.0 (△), 3.0 (□), 3.5 (▽), or 4.0 M urea (◇) or in the absence of urea (○). (B) Pressure-induced denaturation of F29W TnC in the Ca^{2+}-bound state in the presence of 4.0 (■), 5.0 (▲), 5.5 (●), 6.0 (▼), or 7.0 M urea (◆) or in the absence of urea (○).

In Figure 6, we evaluate the unfolding of the Ca^{2+}-bound form of F29W TnC upon addition of urea, using high-pressure NMR. The maintenance of the well-dispersed peaks in the HSQC spectra indicates that the F29W TnC structure was only weakly perturbed by increasing pressure (Figure 6, top), confirming our spectroscopic measurements (Figure 5B). Although we observed the disappearance of some peaks and a reduction in intensity at 5 and 7 M urea at 1 bar, the peak dispersion was essentially the same as those obtained in the absence of urea. However, upon combining 5 or 7 M urea (Figure 6, middle or bottom, respectively) with high hydrostatic pressure, we observed the disappearance of all well-dispersed peaks and the appearance of the overlapped region in the middle of the spectra; these results confirm that the F29W TnC Ca^{2+}-bound form reached the unfolded state. These observations are consistent with the center of spectral mass values (Figure 5B).

From the pressure−denaturation curves of panels A and B of Figure 5 (conducted in the presence of urea), we calculated the volume changes (ΔV) of F29W TnC folding using eq 3 (see Experimental Procedures). The values obtained are listed in Table 3. As observed with the isolated N-domain,[33] ΔV for F29W TnC increased with urea concentration. In addition, the ΔV for folding of the F29W TnC apo form (44.9 mL/mol) was similar to the value obtained for the isolated N-domain (48.6 mL/mol). However, in the presence of Ca^{2+}, the calculated ΔV of F29W TnC was lower than the value for the isolated N-domain.

The free energy change of folding at atmospheric pressure (ΔG°_{atm}) was obtained from eq 5, using the volume changes shown in bold in Table 3 and ΔG° at 1241 bar in the absence of urea ($\Delta G^{\circ 0M}{}_{1241}$) (Figure 7 and Table 4). Table 4 displays the ΔG°_{atm} values for F29W TnC and the F29W/N-domain (residues 1−90)[33] in the presence or absence of Ca^{2+}. The value of ΔG°_{atm} obtained in the absence of Ca^{2+} indicates that the C-domain has a smaller effect on the N-domain structure. Conversely, the value of ΔG°_{atm} obtained in the presence of Ca^{2+} confirms that the thermodynamic stability of the N-domain decreases when the C-domain is attached (Table 4).

■ DISCUSSION

TnC is one of the most studied proteins in the EF-hand family. The factors that determine the affinity and selectivity of sites I−IV for Ca^{2+} have been investigated extensively. The site affinity is affected by more than just the amino acid composition of the Ca^{2+}-binding loop.[17,48,49] There is an inverse correlation between protein stability and the affinity for Ca^{2+}. The C-domain has two high-affinity sites and is very unstable in the apo state, while the N-domain has two low-affinity sites for Ca^{2+} and exhibits high structural stability.[21,49,50] Furthermore, an increase in protein stability induces a decrease in Ca^{2+} affinity.[22,49] In particular, the early work by Tsalkova and

dx.doi.org/10.1021/bi301139d | Biochemistry 2013, 52, 28−40

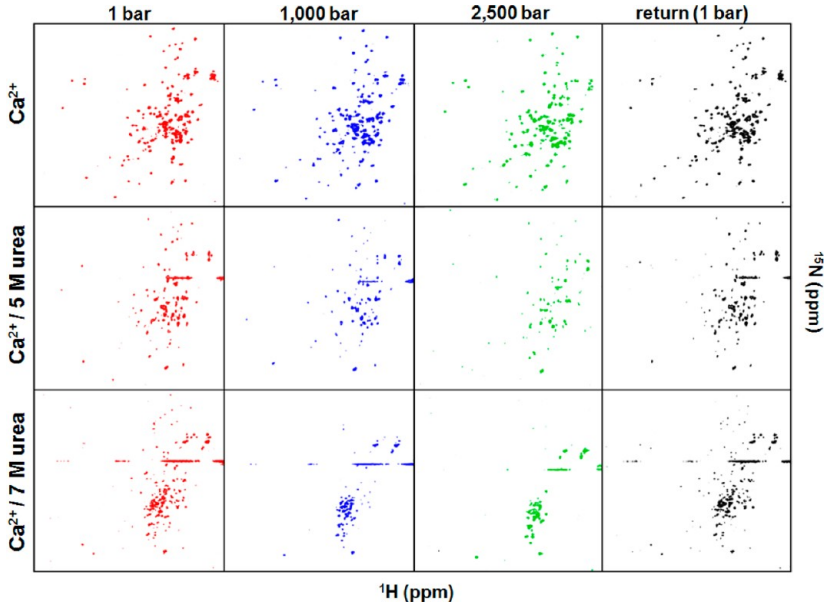

Figure 6. Structural information for the F29W TnC Ca^{2+}-bound state under high-pressure NMR. HSQC spectra of F29W TnC in the presence of 2.1 mM $CaCl_2$, in the presence or absence of 5 or 7 M urea. HSQC spectra are shown over ranges of 6−11 ppm in the ^1H dimension and of 104−132 ppm in the ^{15}N dimension. Red, blue, green, and black cross-peaks correspond to $^1H-^{15}N$ correlations at 1, 1000, and 2500 bar and after pressure release, respectively.

Table 3. ΔV Values of Folding for the F29W/N-Domain and F29W TnC in the Apo and Ca^{2+}-Bound States[a]

	ΔV (mL/mol) with 2.1 mM $CaCl_2$			ΔV (mL/mol) with EGTA	
[urea] (M)	F29W/N-domain[33]	F29W TnC	[urea] (M)	F29W/N-domain[33]	F29W TnC
5.0	36.74 ± 0.76	25.89 ± 1.07	2.0	30.19 ± 0.69	21.31 ± 0.28
5.5	36.60 ± 1.40	39.44 ± 1.09	2.5	38.13 ± 1.73	–
6.0	46.39 ± 1.12	44.08 ± 1.25	3.0	44.24 ± 1.68	27.11 ± 1.29
7.0	59.59 ± 0.73	**47.69 ± 0.50**	3.5	**48.62 ± 2.03**	34.52 ± 0.99
8.0	**60.65 ± 3.95**	–	4.0	–	**44.90 ± 1.58**

[a]Pressure (1−3000 bar) was applied in steps at each urea concentration, and the extent of reaction (α_p, from the change in the center of mass) was plotted according to eq 3 (Experimental Procedures) to obtain ΔV.

Privalov[50] used differential scanning calorimetry to provide evidence that C-domains unfold at lower temperatures than N-domains; they also demonstrated that there were interdomain interactions between the N- and C-domains.

In recent studies, we established a new correlation between Ca^{2+} affinity and thermodynamic stability.[24,33] Following Ca^{2+} binding, the C-domain experiences an increase in stability; this increase is 50% greater than the increase in stability of the N-domain after Ca^{2+} binding. Thus, we proposed that part of the affinity for Ca^{2+} is derived from the free energy change of folding that occurs when Ca^{2+} binds to sites in TnC.

In this report, we analyzed the thermodynamic stability and the structural changes of intact TnC, using a fluorescent mutant, in which Phe 29 was replaced with Trp. This residue is located in the N-domain.

As observed in Figure 4A, Ca^{2+} binding induced a small blue shift and a 3-fold increase in Trp 29 emission. These spectral changes were also observed in the isolated N-domain[33] (F29W/N-domain) and indicate that the Trp residue was less exposed to the solvent, which was followed by relief of some internal quenching. Additionally, as revealed by SAXS (Figure 2), binding of Ca^{2+} also affects the structure of the central helix that connects the N- and C-terminal domains. The volume of the central helix decreases (Figure 2A,B,E), and the helix likely gains rigidity and stability following Ca^{2+} binding. Ca^{2+} also markedly stabilizes the structure of the N- and C-domains (Figures 2B and 4B). However, this effect is different for each domain of intact TnC. The highest urea concentration (8 M) displaces the Trp emission of F29W TnC to red by decreasing the emission by 270 cm^{-1}, which corresponds to 31% of the change induced by 7 M urea and pressure (Figure 5B). SAXS reconstructions confirmed this structural change observed in the presence of Ca^{2+} and 7 M urea; the R_g of F29W TnC (Table 1) and the hypothetical circumferences of the N-domain (Figure 2E) were affected by 7 M urea, even in the presence of Ca^{2+}. Interestingly, this behavior is not observed by fluorescence spectroscopy when intact TnC (F105W) or its isolated N- and C-domains (F29W/N-domain and F105W/C-domain, respectively) are used. For these proteins, the center of spectral mass at 1 bar remains unchanged with urea alone, suggesting that 8 M urea has no effect on the structure of the Ca^{2+}-bound proteins[24,33] (Figure 4B). Globally, these results indicate that in the Ca^{2+}-bound state, the presence of the N-domain does not influence the stability of the C-domain.[24] However, the C-domain significantly affects the thermodynamic stability of the N-domain.

In panels A and B of Figure 5, we demonstrated that high hydrostatic pressure induces a small decrease in the center of spectral mass for F29W TnC; this was observed even in the absence of Ca^{2+}. These results are completely different from

dx.doi.org/10.1021/bi301139d | Biochemistry 2013, 52, 28−40

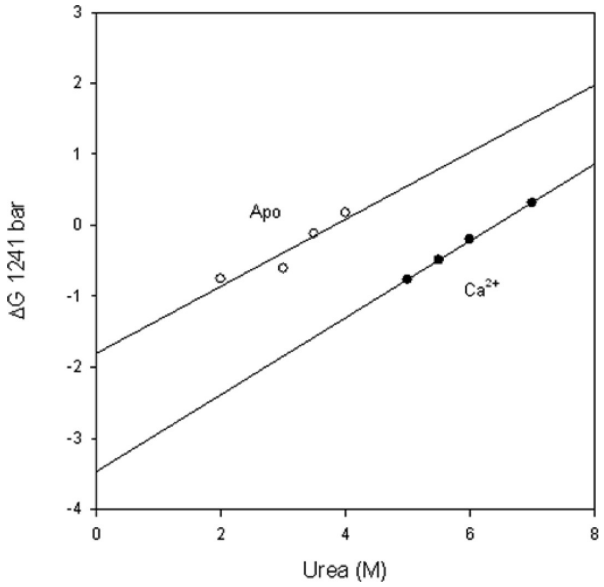

Figure 7. Assessing the free energy change following denaturation of intact F29W TnC in the absence of urea. The $\Delta G^{\circ(U)}_{1241}$ values at 1241 bar were obtained from panels A and B of Figure 5 according to eq 3 and are shown in the presence of 2.1 mM $CaCl_2$ (●) or in the absence of $CaCl_2$ (○). The ΔG° at 1241 bar in the absence of urea was obtained by extrapolation of these curves to the *y*-axis (Table 4).

those observed for F105W TnC and the F105W/C-domain. In the absence of divalent cations, the center of spectral mass decreases under pressure, suggesting that the C-domain is denatured.[24] These results confirm the decreased stability of the apo form of the C-domain when compared with that of the apo form of the N-domain. As presented here and as observed for the isolated N-domain[33] (F29W/N-domain), the complete unfolding of the F29W TnC apo form was achieved only when high pressure was combined with different concentrations of urea. At 3.1 kbar and in the presence of 4 M urea, the center of spectral mass reached 28398 cm^{-1}, a value that is close to the maximum observed for free Trp in solution.[23] This decrease in the center of spectral mass is compatible with denaturation of the N-domain.

With regard to the center of mass of the F29W TnC Ca^{2+}-bound form, we also observed only a small decrease in the center of mass with an increase in pressure. Thus, pressure alone has minimal effects on TnC structure. This conclusion was confirmed by high-hydrostatic pressure NMR using the F29W TnC Ca^{2+}-bound form. Using this technique, we observed similar cross-peaks at 1, 1000, and 2500 bar (Figure 6). Only when we combined high pressure with different concentrations of urea were we able to obtain a center of spectral mass (28302 cm^{-1}) that was compatible with complete unfolding of the F29W TnC Ca^{2+}-bound form. To achieve this center of spectral mass, we had to add 5 M urea. The complete denaturation of the protein induced by pressure combined with high concentrations of urea (5 and 7 M) was confirmed by the disappearance of the cross-peaks and the appearance of the overlapped regions in the middle of the HSQC spectra (Figure 6).

We compare the ΔV of folding for F29W TnC (this study) with the ΔV for the F29W/N-domain in Table 3.[33] In the absence of Ca^{2+}, the calculated ΔV for the intact protein was almost identical to that observed for the isolated N-domain. Under these conditions, as confirmed by the ΔG°_{atm} values (Table 4), the C-domain of TnC had almost no effect on the structure of the N-domain. However, this result was not observed in the presence of Ca^{2+}. The data obtained by SAXS and fluorescence spectroscopy showed that there was intramolecular coupling between the N- and C-domains in the presence of Ca^{2+}. The calculated ΔV for F29W TnC in the presence of Ca^{2+} was smaller than that obtained for the isolated N-domain (Table 3). Additionally, the value of ΔG°_{atm} obtained in the presence of Ca^{2+} indicates that the C-domain destabilizes the structure of the N-domain (Table 4). These observations are complementary to those of Moncrieffe.[29] Using a single Trp mutant of chicken skeletal TnC (F78W), these authors show the midpoints of temperature denaturation curves using circular dichroism data, when the apo form or the protein in the presence of Ca^{2+} or Mg^{2+} was utilized. In their report, they had to guess which transition corresponded to the N-terminus and which corresponded to the C-terminus. However, they suggested that binding of Ca^{2+} to the C-terminal domain destabilizes the N-domain when sites I and II are empty. Here, we observed that this effect also occurred when sites I and II were occupied by Ca^{2+}. The thermodynamic barriers for folding of the isolated N- and C-domains and within the intact protein (F29W and F105W) in the presence or absence of Ca^{2+} are shown in Figure 8. These barriers

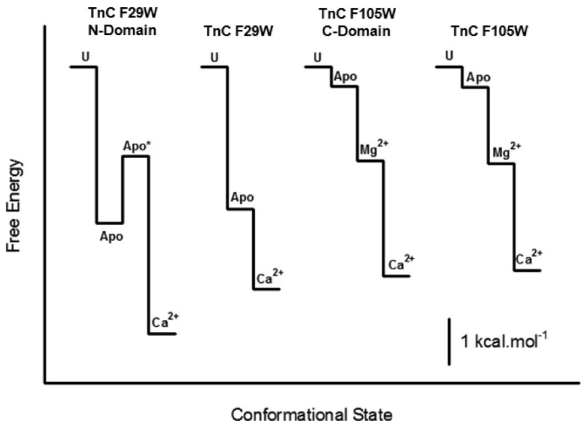

Figure 8. Free energy change for folding of the F29W/N-domain[33] and F29W TnC at atmospheric pressure and 20 °C. apo* corresponds to the free energy change related to the conformational change that precedes Ca^{2+} binding.[63]

Table 4. Values of ΔG° at 1241 bar, ΔG°_{atm}, and $\Delta\Delta G^\circ_{atm}$ for the F29W/N-Domain and F29W TnC[a]

	ΔG° (kcal/mol) (1241 bar)		ΔG°_{atm} (kcal/mol)		
	Ca^{2+}	apo	Ca^{2+}	apo	$\Delta\Delta G^\circ_{atm}$
F29W/N-domain[33]	−4.07 ± 0.38	−1.99 ± 0.18	−5.82 ± 0.50	−3.40 ± 0.24	−2.42
F29W TnC	−3.47 ± 0.06	−1.81 ± 0.40	−4.85 ± 0.08	−3.11 ± 0.45	−1.74

[a] $\Delta\Delta G^\circ_{atm}$ was calculated by subtracting the value for ΔG°_{atm} of the apo form from that of the Ca^{2+}-bound form. The temperature was 20 °C.

dx.doi.org/10.1021/bi301139d | *Biochemistry* 2013, 52, 28−40

summarize all of the results obtained using high hydrostatic pressure and various concentrations of urea; additionally, they show that the N-domain structure is affected by the presence of the C-domain when Ca^{2+} is bound to EF-hand sites.

Finally, we show the plot of $\Delta\Delta G^{\circ}_{atm}$ between the apo and Ca^{2+}-bound states versus pCa_{50} for TnC in Figure 9. In this

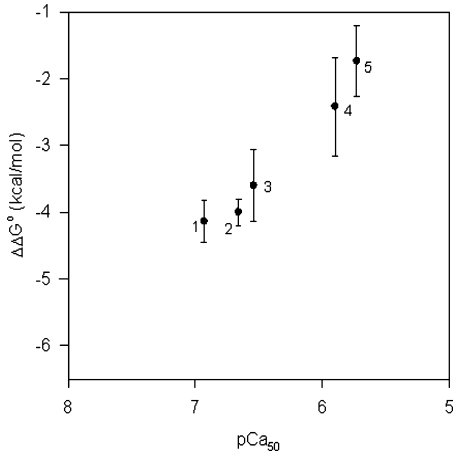

Figure 9. Plot of $\Delta\Delta G^{\circ}_{atm}$ for the apo and Ca^{2+}-bound states vs pCa_{50} for different TnC Trp mutants. The values of ΔG°_{atm} and pCa_{50} for F105W TnC, the F105W/C-domain, and the F29W/N-domain are from ref 33: (1) F105W/C-domain (20 °C), (2) F105W TnC (20 °C), (3) F29W/N-domain (1 °C), (4) F29W/N-domain (20 °C), and (5) F29W TnC (20 °C). The $\Delta\Delta G^{\circ}_{atm}$ value for intact F29W TnC was calculated from ΔG°_{atm} in Table 3, and the pCa_{50} value was from ref 26.

figure, we introduce a data point for F29W TnC (point 5) using the obtained $\Delta\Delta G^{\circ}_{atm}$ value and the average pCa_{50} for F29W TnC calculated from five different studies.[19,25,26,33,51] Again, we observe a strong correlation between the processes of protein folding and binding of Ca^{2+}. As expected, the decrease in $\Delta\Delta G^{\circ}_{atm}$ observed for F29W TnC was accompanied by a slight decrease in Ca^{2+} affinity. Several proteins in addition to troponins have been described to be stabilized by calcium binding, especially when probed by pressure.[52−54]

In summary, the binding of Ca^{2+} and Mg^{2+} to sites III and IV has opposite effects on the structure of the N-domain. The thermodynamic stability of the N-domain increases when Mg^{2+} is bound to the C-domain[29] and decreases when sites III and IV are occupied by Ca^{2+}, even when Ca^{2+} is bound to sites I and II (ref 29 and our results). In the presence of Ca^{2+}, we also observed that the C-domain affects the affinity of the N-domain for Ca^{2+}. This intramolecular coupling observed between the N- and C-domains for the isolated TnC subunit upon the binding of Ca^{2+} may also increase the overall stability of the entire troponin complex (TnC, TnI, and TnT), as shown by a classical differential scanning calorimetry study of the isolated cardiac Tn complex,[55] and may trigger muscle contraction. However, it is not clear how the cross-talk between the N- and C-domains might occur. One possibility involves bending or "melting" of the central helix, which has been observed in the absence of Ca^{2+} when TnI is present.[56,57] Even in the isolated protein, binding of Ca^{2+} to the N-domain induces conformational changes in the C-domain, consistent with communication between these two regions.[58] Thus, a reciprocal transfer of information may occur from the C-domain of TnC to the N-domain. In fact, Trp residues engineered into the N-domain (e.g., F52W and F78W) respond to the binding of a divalent cation to the C-domain.[28,29] Previous studies have identified drugs that bind to the C-domain and change the Ca^{2+} sensitivity of the N-domain.[59] Communication between the N- and C-domains may be particularly important functionally when all four sites are loaded with Ca^{2+}; Förster resonance electron transfer studies demonstrate that the N-domain opens and becomes quite rigid.[28] Here, by construction of low-resolution 3D models using SAXS data, we observed that the central helix becomes thinner and likely more rigid and stable upon Ca^{2+} binding. These changes may affect the cross-talk between the N- and C-domains.

Some parallels can be established with calmodulin. Interactions between the N- and C-terminal domains of mutant calmodulins from *Drosophila melanogaster* have been identified by circular dichroism.[60] In another study, an interdomain linker leads to an increase in the thermostability of calmodulin and decreases the calcium affinity of the calmodulin N-domain.[61]

The C-domain of TnC could modulate the muscle contractile response utilizing fluctuations in Ca^{2+} and Mg^{2+} concentrations, which has been observed in fatigue and hypoxia, for example.[62]

■ ASSOCIATED CONTENT

Supporting Information

Raw scattered intensity $[I(q)]$ plot subtracted from buffer contribution (Figure S1), Guinier plot obtained by ln I versus q^2 (Figure S2), size distribution by DLS for the same conditions studied by SAXS (Figure S3), and the superimposed molecular envelope of the apo form treated with 4 M urea and the TnC crystal structure (Figure S4). This material is available free of charge via the Internet at http://pubs.acs.org.

■ AUTHOR INFORMATION

Corresponding Author

*Instituto de Bioquímica Médica, Instituto Nacional de Biologia Estrutural e Bioimagem, Centro Nacional de Ressonância Magnética Nuclear Jiri Jonas, UFRJ, 21941-590 Rio de Janeiro, RJ, Brazil. E-mail: jerson@bioqmed.ufrj.br (J.L.S.) or mcarvalhosuarez@yahoo.com.br (M.C.S.). Telephone: (55) 21 2562-6756.

Funding

This work was supported by grants from Conselho Nacional de Desenvolvimento Científico e Tecnológico (CNPq), Fundação Carlos Chagas Filho de Amparo à Pesquisa do Estado do Rio de Janeiro (FAPERJ), Ministério da Saúde (MS/DECIT), and Financiadora de Estudos e Projetos (FINEP) of Brazil and the Brazilian Synchrotron Light Laboratory (LNLS) under Proposals SAXS1-11698 and SAXS1-12664.

Notes

The authors declare no competing financial interest.

■ ACKNOWLEDGMENTS

We thank Drs. Lawrence B. Smillie and Joyce R. Pearlstone (University of Alberta, Edmonton, AB) and Dr. Shaker Chuck Farah for donating plasmids and for helpful suggestions. We are grateful to Emerson R. Gonçalves and Santiago Francisco da Silva Alonso for their technical assistance.

REFERENCES

(1) Herzberg, O., and James, M. N. G. (1985) Structure of the calcium regulatory muscle protein troponin C at 2.8 Å resolution. *Nature 313*, 653−659.

(2) Sundaralingam, M., Bergstrom, R., Strasburg, G., Rao, S. T., Roychowdhury, P., Greaser, M., and Wang, B. C. (1985) Molecular structure of troponin C from chicken skeletal muscle at 3-angstrom resolution. *Science 227*, 945−948.

(3) Herzberg, O., Moult, J., and James, M. N. G. (1986) A model for the Ca^{2+}-induced conformational transition of troponin C. A trigger for muscle contraction. *J. Biol. Chem. 261*, 2638−2644.

(4) Satyshur, K. A., Rao, S. T., Pyzalska, D., Drendel, W., Greaser, M., and Sundaralingam, M. (1988) Refined structure of chicken skeletal muscle troponin C in the two calcium state at 2 Å resolution. *J. Biol. Chem. 263*, 1628−1647.

(5) Slupsky, C. M., Reinach, F. C., Smillie, L. B., and Sykes, B. D. (1995) Solution secondary structure of calcium-saturated troponin C monomer determined by multidimensional heteronuclear NMR spectroscopy. *Protein Sci. 4*, 1279−1290.

(6) Houdusse, A., Love, M. L., Dominguez, R., Grabarek, Z., and Cohen, C. (1997) Structures of four Ca^{2+}-bound troponin C at 2.0 Å resolution: Further insights into the Ca^{2+}-switch in the calmodulin superfamily. *Structure 5*, 1695−1711.

(7) Potter, J. D., and Gergely, J. (1975) The calcium and magnesium binding sites on troponin and their role in the regulation of myofibrillar adenosine triphosphatase. *J. Biol. Chem. 250*, 4628−4633.

(8) Hincke, M. T., McCubbin, W. D., and Kay, C. M. (1978) Calcium-binding properties of cardiac and skeletal troponin C as determined by circular dichroism and ultraviolet difference spectroscopy. *Can. J. Biochem. 56*, 384−395.

(9) Johnson, J. D., Collins, J. H., Robertson, S. P., and Potter, J. D. (1980) A fluorescent probe study of Ca^{2+} binding to the Ca^{2+}-specific sites of cardiac troponin and troponin C. *J. Biol. Chem. 255*, 9635−9640.

(10) Andersson, T., Drakenberg, T., Forsén, S., and Thulin, E. (1981) A ^{43}Ca NMR and ^{25}Mg NMR study of rabbit skeletal muscle troponin C: Exchange rates and binding constants. *FEBS Lett. 123*, 39−43.

(11) Braga, C. A., Pinto, J. R., Valente, A. P., Silva, J. L., Sorenson, M. M., Foguel, D., and Suarez, M. C. (2006) Ca^{2+} and Mg^{2+} binding to weak sites of TnC C-domain induces exposure of a large hydrophobic surface that leads to loss of TnC from the thin filament. *Int. J. Biochem. Cell Biol. 38*, 110−122.

(12) Haiech, J., Kilhoffers, M. C., Lukas, T. J., Craig, T. A., Roberts, D. M., and Watterson, D. M. (1991) Restoration of the calcium binding activity of mutant calmodulins toward normal by the presence of a calmodulin binding structure. *J. Biol. Chem. 266*, 3427−3431.

(13) Da Silva, A. C. R., and Reinach, F. C. (1991) Calcium binding induces conformational changes in muscle regulatory proteins. *Trends Biochem. Sci. 16*, 53−62.

(14) Gagné, S. M., Li, M. X., and Sykes, B. D. (1997) Mechanism of direct coupling between binding and induced structural change in regulatory calcium binding proteins. *Biochemistry 36*, 4386−4392.

(15) Golosinska, K., Pearlstone, J. R., Borgford, T., Oikawa, K., Kay, C. M., Carpenter, M. R., and Smillie, L. B. (1991) Determination of and corrections to sequences of turkey and chicken troponins-C. Effects of Thr-130 to Ile mutation on Ca^{2+} affinity. *J. Biol. Chem. 266*, 15797−15809.

(16) Chandra, M., da Silva, E. F., Sorenson, M. M., Ferro, J. A., Pearlstone, J. R., Nash, B. E., Borgford, T., Kay, C. M., and Smillie, L. B. (1994) The effects of N helix deletion and mutant F29W on the Ca^{2+} binding and functional properties of chicken skeletal muscle troponin. *J. Biol. Chem. 269*, 14988−14994.

(17) Grabarek, Z., Tan, R. Y., Wang, J., Tao, T., and Gergely, J. (1990) Inhibition of mutant troponin C activity by an intra-domain disulphide bond. *Nature 345*, 132−135.

(18) Fujimori, K., Sorenson, M. M., Herzberg, O., Moult, J., and Reinach, F. C. (1990) Probing the calcium-induced conformational transition of troponin C with site-directed mutants. *Nature 344*, 182−184.

(19) Pearlstone, J. R., Borgford, T., Chandra, M., Oikawa, K., Kay, C. M., Herzberg, O., Moult., J., Herklotz, A., Reinach, F. C., and Smillie, L. B. (1992) Construction and characterization of a spectral probe mutant of troponin C: Application to analyses of mutants with increased Ca^{2+} affinity. *Biochemistry 31*, 6545−6553.

(20) Da Silva, A. C. R., Araujo, A. H. B., Herzberg, O., Moult, J., Sorenson, M. M., and Reinach, F. C. (1993) Troponin-C mutants with increased calcium affinity. *Eur. J. Biochem. 213*, 599−604.

(21) Fredricksen, R. S., and Swenson, C. A. (1996) Relationship between stability and function for isolated domains of troponin C. *Biochemistry 35*, 14012−14026.

(22) Suarez, M. C., Machado, C. J. V., Lima, L. M. T. R., Smillie, L. B., Pearlstone, J. R., Silva, J. L., Sorenson, M. M., and Foguel, D. (2003) Role of hydration in the closed-to-open transition involved in Ca^{2+} binding by troponin C. *Biochemistry 42*, 5522−5530.

(23) Lakowicz, J. R. (1999) *Principles of fluorescence spectroscopy*, 2nd ed., Springer Publishing, New York.

(24) Rocha, C. B., Suarez, M. C., Yu, A., Ballard, L., Sorenson, M. M., Foguel, D., and Silva, J. L. (2008) Volume and free energy of folding for troponin C C-domain: Linkage to ion binding and N-domain interaction. *Biochemistry 47*, 5047−5058.

(25) Trigo-Gonzalez, G., Racher, K., Burtnick, L., and Borgford, T. (1992) A comparative spectroscopic study of tryptophan probes engineered into high- and low-affinity domains of recombinant chicken troponin C. *Biochemistry 31*, 7009−7015.

(26) Li, M. X., Chandra, M., Pearlstone, J. R., Racher, K. I., Gonzalez, G. T., Borgford, T., Kay, C. M., and Smillie, L. B. (1994) Properties of isolated recombinant N and C domains of chicken troponin C. *Biochemistry 33*, 917−925.

(27) Chandra, M., McCubbin, W. D., Oikawa, K., Kay, C. M., and Smillie, L. B. (1994) Ca^{2+}, Mg^{2+}, and troponin I inhibitory peptide binding to a Phe-154 to Trp mutant of chicken skeletal muscle troponin C. *Biochemistry 33*, 2961−2969.

(28) She, M., Dong, W. J., Umeda, P. K., and Cheung, H. C. (1998) Tryptophan mutants of troponin C from skeletal muscle: An optical probe of the regulatory domain. *Eur. J. Biochem. 252*, 600−607.

(29) Moncrieffe, M. C., Venyaminov, S. Y., Miller, T. E., Guzman, G., Potter, J. D., and Prendergast, F. G. (1999) Optical spectroscopic characterization of single tryptophan mutants of chicken skeletal troponin C: Evidence for interdomain interaction. *Biochemistry 38*, 11973−11983.

(30) Davis, J. P., Rall, J. A., Reiser, P. J., Smillie, L. B., and Tikunova, S. B. (2002) Engineering competitive magnesium binding into the first EF-hand of skeletal troponin C. *J. Biol. Chem. 277*, 49716−49726.

(31) Yu, A., Ballard, L., Smillie, L. B., Pearlstone, J., Foguel, D., Silva, J., Jonas, A., and Jonas, J. (1999) Effects of high pressure and temperature on the wild-type and F29W mutant forms of the N-domain of avian troponin C. *Biochim. Biophys. Acta 1431*, 53−63.

(32) Pearson, D. S., Swartz, D. R., and Geeves, M. A. (2008) Fast pressure jumps can perturb calcium and magnesium binding to troponin C F29W. *Biochemistry 47*, 12146−12158.

(33) Suarez, M. C., Rocha, C. B., Sorenson, M. M., Silva, J. L., and Foguel, D. (2008) Free-energy linkage between folding and calcium binding in EF-hand proteins. *Biophys. J. 95*, 4820−4828.

(34) Svergun, D. I. (1992) Determination of the regularization parameter in indirect-transform methods using perceptual criteria. *J. Appl. Crystallogr. 25*, 495−503.

(35) Svergun, D. I., Petoukhov, M. V., and Koch, M. H. (2001) Determination of domain structure of proteins from X-ray solution scattering. *Biophys. J. 80*, 2946−2953.

(36) Volkov, V. V., and Svergun, D. I. (2003) Uniqueness of ab initio shape determination in small-angle scattering. *J. Appl. Crystallogr. 36*, 860−864.

(37) Kozin, M. B., and Svergun, D. I. (2001) Automated matching of high- and low-resolution structural models. *J. Appl. Crystallogr. 34*, 33−41.

(38) Paladini, A. A., and Weber, G. (1981) Pressure-induced reversible dissociation of enolase. *Biochemistry 20*, 2587−2593.

(39) Silva, J., and Weber, G. (1993) Pressure stability of proteins. *Annu. Rev. Phys. Chem. 44*, 89−113.
(40) Mertens, H. D., and Svergun, D. I. (2010) Structural characterization of proteins and complexes using small-angle X-ray solution scattering. *J. Struct. Biol. 172*, 128−141.
(41) Doniach, S. (2001) Changes in biomolecular conformation seen by small angle X-ray scattering. *Chem. Rev. 101*, 1763−1778.
(42) Svergun, D. I. (1999) Restoring low resolution structure of biological macromolecules from solution scattering using simulated annealing. *Biophys. J. 76*, 2879−2886.
(43) Silva, J. L., Oliveira, A. C., Gomes, A. M., Lima, L. M., Mohana-Borges, R., Pacheco, A. B., and Foguel, D. (2002) Pressure induces folding intermediates that are crucial for protein-DNA recognition and virus assembly. *Biochim. Biophys. Acta 1595*, 250−265.
(44) Panick, G., Vidugiris, G. J., Malessa, R., Rapp, G., Winter, R., and Royer, C. A. (1999) Exploring the temperature-pressure phase diagram of staphylococcal nuclease. *Biochemistry 38*, 4157−4164.
(45) Silva, J. L., Foguel, D., and Royer, C. A. (2001) Pressure provides new insights into protein folding, dynamics and structure. *Trends Biochem. Sci. 26*, 612−618.
(46) Foguel, D., and Silva, J. L. (2004) New insights into the mechanisms of protein misfolding and aggregation in amyloidogenic diseases derived from pressure studies. *Biochemistry 43*, 11361−11370.
(47) Meersman, F., Dobson, C. M., and Heremans, K. (2006) Protein unfolding, amyloid fibril formation and configurational energy landscapes under high pressure conditions. *Chem. Soc. Rev. 35*, 908−917.
(48) Reid, R. E., Gariépy, J., Saund, A. K., and Hodges, R. S. (1981) Calcium-induced protein folding. Structure-affinity relationships in synthetic analogs of the helix-loop-helix calcium binding unit. *J. Biol. Chem. 256*, 2742−2751.
(49) Grabarek, Z., Mabuchi, Y., and Gergely, J. (1995) Properties of troponin C acetylated at lysine residues. *Biochemistry 34*, 11872−11881.
(50) Tsalkova, T. N., and Privalov, P. L. (1980) Stability of troponin C. *Biochim. Biophys. Acta 624*, 196−204.
(51) Leblanc, L., Bennet, A., and Borgford, T. (2000) Calcium affinity of regulatory sites in skeletal troponin-C is attenuated by N-cap mutations of helix C. *Arch. Biochem. Biophys. 384*, 296−304.
(52) Bonafe, C. F., Villas-Boas, M., Suarez, M. C., and Silva, J. L. (1991) Reassembly of a large multisubunit protein promoted by nonprotein factors. Effects of calcium and glycerol on the association of extracellular hemoglobin. *J. Biol. Chem. 266*, 13210−13216.
(53) Bonafe, C. F., Araujo, J. R., and Silva, J. L. (1994) Intermediate states of assembly in the dissociation of gastropod hemocyanin by hydrostatic pressure. *Biochemistry 33*, 2651−2660.
(54) Somkuti, J., Bublin, M., Breiteneder, H., and Smeller, L. (2012) Pressure-Temperature Stability, Ca^{2+} Binding, and Pressure-Temperature Phase Diagram of Cod Parvalbumin: Gad m1. *Biochemistry 51*, 5903−5911.
(55) Jacobson, A. L., Devin, G., and Braun, H. (1981) Thermal denaturation of beef cardiac troponin and its subunits with and without calcium ion. *Biochemistry 20*, 1694−1701.
(56) Vassylyev, D. G., Takeda, S., Wakatsuki, S., Maeda, K., and Maéda, Y. (1998) Crystal structure of troponin C in complex with troponin I fragment at 2.3-Å resolution. *Proc. Natl. Acad. Sci. U.S.A. 95*, 4847−4852.
(57) Vinogradova, M. V., Stone, D. B., Malanina, G. G., Karatzaferi, C., Cooke, R., Mendelson, R. A., and Fletterick, R. J. (2005) Ca^{2+}-regulated structural changes in troponin. *Proc. Natl. Acad. Sci. U.S.A. 102*, 5038−5043.
(58) Wang, X., Li, M. X., Spyracopoulos, L., Beier, N., Chandra, M., Solaro, R. J., and Sykes, B. D. (2001) Structure of the C-domain of Human Cardiac Troponin C in Complex with the Ca^{2+} Sensitizing Drug EMD 57033. *J. Biol. Chem. 276*, 25456−25466.
(59) Grabarek, Z., Leavis, P. C., and Gergely, J. (1986) Calcium binding to the low affinity sites in troponin C induces conformational changes in the high affinity domain. A possible route of information transfer in activation of muscle contraction. *J. Biol. Chem. 261*, 608−613.
(60) Maune, J. F., Beckingham, K., Martin, S. R., and Bayley, P. M. (1992) Circular dichroism studies on calcium binding to two series of Ca^{2+} binding site mutants of *Drosophila melanogaster* calmodulin. *Biochemistry 31*, 7779−7786.
(61) Sorensen, B. R., Faga, L. A., Hultman, R., and Shea, M. A. (2002) An interdomain linker increases the thermostability and decreases the calcium affinity of the calmodulin N-domain. *Biochemistry 41*, 15−20.
(62) Headrick, J. P., and Willis, R. J. (1991) Cytosolic free magnesium in stimulated, hypoxic, and underperfused rat heart. *J. Mol. Cell. Cardiol. 23*, 991−999.
(63) Foguel, D., Suarez, M. C., Barbosa, C., Rodrigues, J. J., Jr., Sorenson, M. M., Smillie, L. B., and Silva, J. L. (1996) Mimicry of the calcium-induced conformational state of troponin C by low temperature under pressure. *Proc. Natl. Acad. Sci. U.S.A. 93*, 10642−10646.